Published in final edited form as:

Annu Rev Anal Chem (Palo Alto Calif). 2019 June 12; 12(1): 109–128. doi:10.1146/annurev-anchem-061417-125747.

Recent Developments in Nanosensors for Imaging Applications in Biological Systems

Guoxin Rong[1], **Erin E. Tuttle**[2,*], **Ashlyn Neal Reilly**[1,*], **Heather A. Clark**[1,2]

[1]Department of Bioengineering, Northeastern University, Boston, Massachusetts 02115, USA;

[2]Department of Chemistry and Chemical Biology, Northeastern University, Boston, Massachusetts 02115, USA

Abstract

Sensors are key tools for monitoring the dynamic changes of biomolecules and biofunctions that encode valuable information that helps us understand underlying biological processes of fundamental importance. Because of their distinctive size-dependent physicochemical properties, materials with nanometer scales have recently emerged as promising candidates for biological sensing applications by offering unique insights into real-time changes of key physiological parameters. This review focuses on recent advances in imaging-based nanosensor developments and applications categorized by their signal transduction mechanisms, namely, fluorescence, plasmonics, MRI, and photoacoustics. We further discuss the synergy created by multimodal nanosensors in which sensor components work based on two or more signal transduction mechanisms.

Keywords

biosensing; fluorescence; plasmonics; magnetic resonance imaging; MRI; photoacoustics; multimodal

INTRODUCTION

The living system works as a complex supramolecular machine modulated by numerous dynamic biological processes. The fluctuations of biomolecule concentrations and bioactivities not only encode valuable information that helps unravel underlying mechanisms at the molecular level but also have major implications for clinical applications (1). Sensors that can detect and/or monitor analytes or functions in the biological system have played a prominent role in recent years as an essential research tool to answer fundamental questions about the self-regulation of living systems (2). They have also emerged in the commercial domain as integral parts of wearable devices that track vital signs or electrolyte levels in real time (3). Sensors, in broad terms, consist of two components: The first part is a receptor moiety that recognizes the biological target or its biological activity and relays the recognition event to the second part, the signal transduction element, to convert the

h.clark@northeastern.edu.

*These authors contributed equally to this article

recognition event into a measurable readout (4). Ideally, sensors suitable for in vivo and in vitro applications should meet the following criteria: dynamic sensing range in line with the physiological range of the analyte of interest; high selectivity against major interferents in the biological environment; good stability during the measurement period; rapid sensor response; and minimum perturbation to the normal biological functions and high biocompatibility. Nanosensors, in particular, have recently emerged as candidates that show great potential to meet many of the stringent requirements mentioned above (5, 6).

Nanosensors, defined in this review as nanoscale constructs or larger sensors that contain nanoscale features, have made promising strides as analytical tools to understand biological functions and provide advantageous sensing properties. Certain types of sensors based on nanoscale platforms can offer a high number of binding sites suitable for different functionalities, whereas in other formats, the active components of the sensors often take advantage of their unique size-dependent physicochemical properties, such as the quantum dot and noble metal nanoparticle (NP). As such, nanosensors have recently been used for in vitro and in vivo applications traditionally dominated by molecular or genetically encoded indicators.

In this review, we focus on the significant advances in nanosensor development applied toward in vitro or in vivo measurements, mostly in the past five years. We follow the lead of Yogi Berra’s immortal words “You can observe a lot by just watching,” which rings especially true to the biosensing community only with a slight tweak: You can observe a lot of biological processes by just watching sensor responses with high spatiotemporal resolutions. Thus, we mostly focus on imaging-based nanosensors and organize the following discussions of nanosensor developments based on four broad imaging-based signal transduction mechanisms: fluorescence-, plasmonics-, magnetic resonance imaging (MRI)-, and photoacoustics (PA)-based sensing. We deliberately exclude the burgeoning fields of electrochemical-based wearable chemical sensors, as they are covered by the excellent review from the Rogers group (7) in this volume. Finally, we briefly touch upon recent developments of nanosensors that involve multiple mechanisms for biological sensing applications.

FLUORESCENCE-BASED NANOSENSORS

Fluorescence-based sensing was one of the earliest adopted techniques to study spatiotemporal dynamics of biomolecules of interest in the living system (8). Since the invention of calcium-sensitive fluorescent dyes by Roger Tsien and coworkers in the late twentieth century (9), molecular indicators (10, 11), together with later developed genetic encoded proteins (12), form the backbone of quantitative sensing and are widely used in the biological science community. However, both molecular fluorescent indicators and fluorescent protein indicators face certain limitations. Molecular probes that enter the intracellular space, facilitated by acetoxymethyl esters, can leach from certain types of cells, sometimes in the matter of minutes (13), therefore significantly limiting the observation time. Meanwhile, genetically encoded indicators could potentially alter the normal biochemical dynamics of the targeted analytes or bioactivities (14). Exogenous fluorescent nanosensors can complement the current palette of indicators, constituting a viable

alternative for elucidating the dynamics of biomolecules and their associated biological functions (15, 16).

Optode-Based Nanosensors

One class of fluorescent nanosensors that has recently drawn increasing attention is optode-based nanosensors (OBNs). Analogous to its electrical counterpart, ion-selective electrodes, the OBN consists of three components: a chelator (ionophore) for target recognition, a pH-sensitive fluorophore (chromoionophore) for signal transduction, and an ionic additive for balancing the charge, all of which are hosted in a polymer matrix. The working principle is straightforward. The ionophore extracts the ion of interest, such as sodium, from the surrounding environment into the sensor matrix, inducing the deprotonation of the chromoionophore to maintain charge-neutrality within the sensor, thus evoking a detectable change in the intensity of the fluorescence. This maturing technique has been applied to detect ions in biofluids (17, 18) and extended to small-molecule targets such as dopamine (19), acetylcholine (20), and histamine (21). The OBN platform offers superb selectivity against major interferents. Moreover, given the decoupling of the recognition and signal transduction moieties, the modular OBN platform enables fine-tuning of the response dynamic range by modifying the components to accommodate different applications. For instance, fluorescent dyes that emit in the near-infrared (NIR) range can be incorporated to the OBN to facilitate in vivo analyte detection (22).

OBNs are suitable for tracking ion level fluctuations, which play a pivotal role in neuroscience. Recently, Clark and coworkers (23) applied OBNs to track intracellular Ca^{2+} dynamics as a baseline study to evaluate the feasibility of OBNs for intracellular ion flux studies (Figure 1a). OBNs with two pH-sensitive fluorophores were fabricated to achieve a ratiometric optical readout that minimizes imaging artifacts and increases the sensitivity compared to single-wavelength OBNs (24). The Ca^{2+} OBNs were introduced into the cytosol of HeLa cells through microinjection to prevent endosomal compartmentalization of the sensors. The OBN fluorescence-intensity ratios were empirically converted into Ca^{2+} concentrations during the pharmacological stimulation, and the response amplitude and kinetics agreed with results obtained from conventional molecular indicators. This work demonstrated that OBNs are capable of tracking intracellular ion flux events. Rong et al. (25) further built on this technology to track intracellular Na^+ dynamics in primary rat dorsal root ganglion (DRG) cells, where Na^+ channels play a major role in modulating excitability of DRG neurons and are crucial to understand the mechanism of neuropathic pain (26). In order to induce Na transients on neurons microinjected with sensors, the authors utilized planar transparent microelectrodes (27) for electrical stimulation instead of conventional patch pipette to reduce mechanical stress on the microinjected cell. They demonstrated for the first time that OBNs have the temporal resolving power to track neuronal Na^+ flux during repetitive pulse train stimulations. Given the broad interest in understanding the regulatory role that Na^+ plays in neuroscience and the lack of choices of Na^+ indicators compared with those of Ca^{2+}, the combination of Na^+ OBN, microinjection, and transparent microelectrodes provides a feasible alternative to existing electrophysiological tools for tracking intracellular Na^+.

Carbon Nanotube–Based Fluorescent Nanosensors

Another promising class of fluorescent nanosensors is based on single-walled carbon nanotubes (SWCNTs). SWCNTs offer unique photophysical properties, including polarized fluorescence emission and stability against photobleaching (28). SWCNTs also have an intrinsic emission centered at the NIR region, which is ideal for in vivo applications. As previously reported, SWCNT fluorescence is sensitive to the binding of nitric oxide (NO) through SWCNT exciton quenching (29). Iverson et al. (30) have demonstrated that DNA-wrapped SWCNTs can track local NO changes induced by inflammation in the liver of a mouse for more than 400 days with minimal signal decay, reflecting a remarkable achievement in fluorescence-based sensing. In one recent study, Kruss et al. (31) demonstrated label-free monitoring of dopamine flux from PC12 neuro-progenitor cells using a SWCNT sensor array. Their approach allows spatiotemporal mapping of dopamine release during K^+ stimulation with high spatial resolution (20,000 sensor/cell), capable of pinpointing the local hotspots of dopamine release sites on the subcellular-length scales.

Quantum Dot–Based Fluorescent Nanosensors

Quantum dots have been routinely used as signal reporters in nanosensors, offering superb photostability compared to organic molecules (32, 33). One reason is that a single quantum dot is comprised of tens of thousands of individual atoms with much more delocalized chemical bonding, increasing its tolerance against photon-induced damaging in contrast to individual fluorescent dye molecules (34). In recent years, quantum dot–based nanosensors have been applied to a variety of in vitro sensing applications (35), such as pH (36), Ca^{2+} (37), and K^+ (38) sensing. For instance, Orte et al. (36) demonstrated for the first time that the photoluminescence decay time of functionalized quantum dots can be used to detect intracellular pH changes when paired with fluorescence lifetime imaging microscopy (FLIM), resulting in improved sensitivity compared to pH fluorescent dyes. In another work, Zamaleeva et al. (37) fabricated an intracellular Ca^{2+} nanosensor by taking advantage of the Förster resonance energy transfer (FRET) between the quantum dot donor and red-emitting CaRuby Ca^{2+} dye acceptor functionalized on the quantum dot surface. This nanoconstruct was further functionalized with cell-penetrating peptides to facilitate cytosolic delivery. The nanosensors were able to resolve cross-membrane Ca^{2+} transients in BHK cells with the temporal resolution of 250 ms during pharmacological stimulation, opening up a new track for probing microdomain Ca^{2+} signaling events.

DNA-Based Fluorescent Nanosensors

Fluorescent nanosensors can also be categorized by their recognition elements. For instance, DNA has been consistently used as the backbone or recognition moiety in sensor designs, as they are modular and highly programmable, enabling molecularly identical assemblies of complex functional structures with minimal variations (39). Numerous nanosensors developed in recent years have used DNA as the integral part of the sensor structure for biological sensing applications, such as for intracellular Cl^- (40), messenger-RNA (mRNA) (41), enzyme catalytic activity (42), and cancer biomarkers (43). For instance, Krishnan and coworkers (40) have fabricated a pH-independent fluorescent DNA nanodevice, termed Clensor, to detect intracellular Cl^- levels in *Drosophila melanogaster* With the targeting

DNA sequence and associated Cl^--sensitive fluorophore and reference fluorophore, Clensor can accurately target and track lumenal lysosomal Cl^- levels with ratiometric signal output (Figure 1b). Another intriguing DNA nanosensor to detect mRNA in single cells was inspired by the anatomical features of the snail. Tay et al. (41) have presented a nano-snail-inspired nucleic acid locator (nano-SNEL) with a molecular beacon for mRNA sensing encapsulated within the protective DNA nanoshell. The novel protective nanoshell design mitigated enzymatic degradation, allowing the sensors to visualize live cell RNA transcription with extended period of time. Two recent studies by the Tan group further demonstrated applications of 3D DNA architectures as nanomachines for targeting cancer biomarkers (44) and mRNAs in live cells (45).

Peptide-Based Fluorescent Nanosensors

Peptides are another biomolecule employed as the recognition moiety in nanosensors. Development of peptide-based nanosensors has been rapidly increasing for detection of disease-related protease activity. In one sensing scheme, peptide-based sensors use fluorophore-tagged peptides immobilized on NP substrates that will be cleaved off by the target protease in the body and then subsequently analyzed after urinal clearance. With this sensor design, common issues related to imaging through the body tissues are circumvented via the transport of the signal reporters out of the body. Lin et al. (46) have successfully demonstrated the feasibility of this sensing scheme by detecting thrombin in mice using iron oxide NPs surface modified with thrombin-sensitive peptides containing conjugated fluorescent reporters. A recent study by Dudani et al. (47) took this approach further by assembling a library of fluorescent nanosensors to detect protease activity to classify prostate cancer based on aggressiveness. The nanosensors were robust in categorizing cancers and outperformed conventionally used serum cancer biomarkers, offering great potential in clinical applications.

Other Emerging Materials for Luminescent Nanosensors

Apart from the common building blocks in fluorescence-based nanosensor design mentioned above, other types of materials are also employed based on their unique photophysical properties to enhance sensor performance. Lanthanide-doped upconversion nanoparticles (UCNPs) exhibita large anti-Stokes shift, converting NIR excitation into emission in the visible wavelength range. This feature enables deeper image penetration depth with minimal photobleaching and fluorescence background from the specimen (48). Liu et al. (49) have leveraged the optical properties of UNCPs to design a FRET sensor and pioneered the monitoring of methylmercury levels in mice by tracking changes in the upconversion luminescence. Gold nanoclusters (AuNCs) are another class of promising luminescent materials, demonstrating high photostability, tunable emission spectra, and large Stokes shift. Recently, Yu et al. (50) have used chitosan-functionalized AuNCs tagged with H_2S-sensitive merocyanine to successfully establish a FRET sensing platform for in vivo detection of endogenous H_2S (Figure 1c). Carbon dots (Cdots) have also become popular sensing components in recent years due to their excellent optical properties and low cytotoxicity (51) and have been applied recently by Cash and coworkers for ionophore-based Na^+ sensing applications (52).

Novel Imaging Approaches for Enhancing Nanosensor Performances

Advances in fluorescence-based imaging modalities have broadened applications for nanosensors by taking advantage of the larger imaging depth, reduced background, and higher spatiotemporal resolution these emerging techniques offer. For instance, recent progresses on both two-photon excitation microscopy (53) and NIR-II imaging (54) enable imaging deep in the tissue with higher spatial resolution than conventional microscopy. This improvement on general imaging capabilities has helped advance nanosensor applications in both in vitro and in vivo biosensing (55–57). Furthermore, FLIM (58) also improved its spatiotemporal resolution in recent years with additional capacity for multichannel imaging (59). This advancement in imaging led to applications of nanomaterials in biological sensing, such as detection of mRNA (60) and hypochlorite (61).

PLASMONICS-BASED NANOSENSORS

Despite advances in fluorescence-based sensing, the technology commonly suffers from limited observation time due to the susceptibility of the sensor to photodamage. Nanosensors based on plasmonic nanomaterials, represented by noble metal NPs, can partially mitigate this concern (62). The optical properties of plasmonic materials referred to in this review are limited to localized surface plasmon resonance (LSPR) or plasmon from the noble metal NPs, which is defined as collective oscillations of free electrons within the NP upon illumination. Compared with fluorescent materials, plasmonic NPs offer larger optical cross sections at the respective resonance wavelengths, whereas individual dye molecules have a finite photon emission rate of approximately 5 kHz, which intrinsically limits signal intensities (63). Moreover, plasmonic NPs have extremely stable optical outputs because the signal is based on light scattering. Thus, the NPs never bleach or blink, enabling long-term, intermittent-free sensing with no limits on observation time, in contrastto organic fluorophores, which can only survive a definite number of excitation/emission cycles (~1×10^6) before eventually bleaching (64). The optical response of plasmonic nanomaterials also depends on the size, geometry, and surrounding environment (65), all of which form the foundation of various plasmonic-based sensing schemes for biological applications (66).

Plasmon Coupling–Based Nanosensors

When two or more noble metal NPs of similar sizes approach each other, their plasmons couple in a distance-dependent manner. The plasmon resonance wavelength red-shifts with decreasing interparticle distances (67). The spectral shift associated with the plasmon coupling becomes most pronounced when interparticle distances are comparable to or smaller than one particle diameter (68). Therefore, plasmon coupling can be used to break the diffraction limit to track distance changes of NP-labeled biomolecules by converting the molecular interactions occurring at the near field to an optical observable at the far field. Plasmon coupling–based nanosensors have been applied to map plasma membrane heterogeneity (69), lateral dynamics of epidermal growth factor receptors on the cancer cell membrane (70), and viral membrane fluidity (71), to name a few applications. Recently, Chen et al. (72) have used preassembled plasmonic NP dimers, termed plasmon rulers, to probe DNA stiffness (Figure 2a). By analyzing the distance-dependent spectral fluctuations of DNA-tethered plasmon rulers, valuable information about the length and conformational

stiffness of both single- and double-stranded DNAs can be obtained. In addition to the spatial information obtained from the spectral shift of plasmon rulers, the polarization of coupled plasmon resonance also encodes additional information about the orientation and chirality of the underlying active structures. Sun et al. (73) have taken advantage of this optical property to sense intracellular telomerase using a DNA-linked gold chiral heterodimer. Quantifying the circular dichroism intensity, this sensing strategy can achieve a linear range for detecting telomeres in single cells down to 1.7×10^{-15} IU and is translatable to other chirality-based schemes.

Plasmonic Enhancing–/Quenching-Based Nanosensors

Plasmons can also concentrate the incident electromagnetic field to modulate the emission from the fluorophores at the vicinity of plasmonic NPs. The subsequent intensity changes via plasmonic enhancement/quenching can be used for analyte detection (74). A plasmonic-modulated optical sensing scheme has recently been employed for detecting intracellular thiols (75), mRNA (76), uranyl (77) and other ions (78). For instance, Xu et al. (75) have fabricated a BODIPY-gold nanoparticle (AuNP) sensor where the BODIPY dyes are quenched due to the FRET and inner filter effect of the AuNP plasmon. The nanosensor exhibits a turn-on fluorescence response as BODIPY molecules are displaced from the AuNP in the presence of thiols that have a stronger binding affinity to the gold surface. The sensor has been successfully applied to intracellular thiol monitoring in HeLa cells. W u et al. (77) further demonstrated for the first time the use of a DNAzyme-AuNP nanosensor for cellular ion monitoring. The DNAzyme was functionalized with thiol at the 3′ end and Cy3 at the 5′ end. In the presence of the ion of interest, the strand containing Cy3 is cleaved off from the AuNP surface, resulting in a turn-on sensor response as the Cy3 fluorescence is no longer quenched by the particle plasmon.

Single Nanoparticle Surface-Enhanced Raman Scattering

Another area of plasmonic-based sensing is surface-enhanced Raman scattering (SERS), where the enhanced electromagnetic field at the NP surface excites normally undetectable vibration modes of targeted molecules. Field enhancement at the NP surface or “hotspots” in carefully designed active plasmonic nanostructures have been applied to label-free chemical sensing (79). Fluorophore molecules can also be added to the particle surface to further enhance the SERS signal of the analyte by introducing additional chemical enhancement. In one notable example, Kircher and coworkers (80) designed chalcogenopyrylium dyes for functionalizing AuNP SERS probes and successfully applied the probes to in vivo cancer biomarker detection with attomolar sensitivity (Figure 2b).

MAGNETIC RESONANCE IMAGING-BASED NANOSENSORS

Both fluorescence- and plasmonic-based nanosensors rely on photons to relay information of the dynamic changes of the underlying analyte or activity. MRI-based nanosensors, on the other hand, rely on the magnetism of superparamagnetic particles, which are magnetic only under an external field, to alter the relaxivity time of nearby water molecules (81). As new research enables the construction of compact permanent magnets with increasingly high field homogeneity, the use of nuclear magnetic resonance (NMR) is no longer constrained

by the need for bulky cryogenically cooled magnets in NMR/MRI instruments (82). Instrumentation will become smaller, more portable, and less expensive to operate, increasing the potential demand for MRI-responsive sensors. MRI-based sensing has several advantages: MRI is not impacted by tissue depth (83), is noninvasive provided suitable delivery mechanisms are found (84), and is not subject to signal decay over time, which is a limitation with fluorescence-based sensors. However, unaided MRI has low sensitivity, requiring the use of contrast agents and other sensitivity-enhancing probes. Nanoscale probes offer many advantages for magnetic-based sensing, such as enhanced permeability and retention (EPR) which leads to greater delivery of the nanomaterials to tumors than normal tissue (85). The core and surface of the nanomaterials are also tunable, facilitating changes to the physicochemical properties (i.e., the magnetic anisotropy energy barrier and hydrophilicity/hydrophobicity) of the sensors to favor certain biochemical interactions (86).

Recent advances in MRI-based nanosensor development for biological use has enabled better understanding of brain functions (87, 88) and metabolic processes (83) and allowed for safer, more accurate medical imaging (89). MRI is a noninvasive and reliable technique, often used in brain imaging but limited by certain challenges. For example, imaging neurotransmitters using MRI is difficult due to rapid changes in concentration and low baseline concentrations of neurotransmitters in the brain. Recently, Luo et al. (87) developed a highly specific nanosensor to image acetylcholine in the brain via MRI. The sensor was comprised of the enzyme butyrylcholinesterase (BuChE) and pH-responsive gadolinium-based contrast agents (GBCAs) coimmobilized on a nanoparticle. BuChE hydrolyzes acetylcholine into choline and acetic acid, generating a localized pH drop that the modified GBCAs detect. In vivo experiments successfully applied the nanoprobe to detect drug-induced acetylcholine release in rat medial prefrontal cortex (Figure 3a).

Although the mechanisms and behaviors of Ca^{2+} as a signaling molecule are not fully understood, abnormal Ca^{2+} patterns have been linked to numerous brain disorders, including Alzheimer′s disease (90). Okada et al. (88) developed magnetic Ca^{2+} -responsive NPs for analyzing real-time Ca^{2+} dynamics in the brain to further understand extracellular Ca^{2+} signaling behavior and elucidate normal and abnormal Ca^{2+} responses. The sensors were designed using both the magnetic NPs and the proteins that are part of natural Ca^{2+} -responsive machinery and sensitive to 0.1–1.0-mM changes in $[Ca^{2+}]$. Fused synaptotagmin monomers, each with two Ca^{2+} -binding sites, were mixed with iron oxide NPs coated with phosphatidylcholine and phos-phatidylserine lipids. Ca^{2+} binding to the proteins induces protein-lipid complex formation with phosphatidylserine, creating NP clusters. As a reduction in $[Ca^{2+}]$ leads to a release of ions from the binding sites and subsequent breakdown of the protein-lipid complex, the NPs will disaggregate at lower concentrations. The sensors successfully detected $[Ca^{2+}]$ dynamics in rat brains (Figure 3b). Reversible magnetic NP clustering is known to magnify small ion concentration fluctuations into readable changes in MRI signals, making the magnetic NP sensors ideal for real-time monitoring using functional MRI.

In addition to advances in small-molecule and ion sensing, novel nanosensors for macromolecule detection have also been developed (91, 92). Zabow et al. (83) have proposed a system for subsurface studies of biological processes using nanosensor

assemblies that operate in NMR radio frequencies. The sensors, composed of stimuli-responsive hydrogel fixed between a pair of magnetic disks, were applied to measure pH as an indicator of the metabolic rate of Madin-Darby canine kidney cells. The design has the potential to be tunable to a variety of biomolecules, as many reactive components can be embedded within the gel matrix, whereas methacrylic acid side groups were used in pH measurements. The pH-sensitive hydrogel was placed between a pair of magnetic disks as a spacer. When exposed to the external MRI fields, water molecules within hydrogel experience a shift in NMR frequencies relative to the distance between the magnetic disks modulated by the pH-sensitive hydrogel spacer (Figure 3c). Arrayed sensors also have the potential for spatial and temporal localization to measure ion gradients using MRI.

Apart from tracking endogenous analytes or activities, real-time monitoring of drug release kinetics has also drawn considerable attention since chemotherapies were first developed (93). The inability to accurately quantify drugs in tissues of interest can lead to under- and overdosing. MRI is an ideal imaging technique for drug monitoring, as the NPs can be spatially located regardless of tissue depth. Liu et al. (94) have prepared a versatile NIR-triggered NP drug delivery and monitoring system using hollow-structure nanocomposites loaded with anticancer drugs. Release of the drugs from the system lowers the longitudinal relaxation time (T_1) signal, meaning that drug release and localization can be monitored in vivo via MRI, as demonstrated using zebrafish.

Although M RI-based nanosensors benefit from superb imaging depth and their effectiveness in boosting the sensitivity of the technique, the ability to noninvasively deliver the sensors to the location of interest is limited. For example, neurotransmitter-targeted sensors require direct delivery to the cerebral spinal fluid as the blood-brain barrier inhibits the delivery of probes administered through traditional injections (95). More invasive means must be used to directly administer the nanosensors to the brain, often requiring surgery. For tumor-targeting systems, the EPR effect offers a twofold increase in selective delivery, a promising yet limited advantage that still requires further enhancement (85).

PHOTOACOUSTICS-BASED NANOSENSORS

PA imaging is another burgeoning imaging technique (96) with deep imaging depth that uses nanosecond laser pulses to cause photon absorption and expansion of the target of interest, emitting ultrasound signals in the process. PA imaging has the combined benefits of both the deep imaging depth of ultrasound and the high image contrast offered by optical imaging (97). Furthermore, the technique is noninvasive and does not cause tissue damage. Contrast agents can further improve the image contrast by clustering in the area of interest. Certain types of NPs are particularly good contrast agents because they have a strong stable PA signal as compared to the weak signals of the surrounding tissue (97). As such, NPs capable of acting as PA-based sensors for biologically important molecules are opening new avenues for in vivo biological sensing.

Currently, PA sensing has been used to detect both Li^+ (98) and K^+ (22). Li^+, which is commonly used in treating bipolar disorder, is a clinically important ion to track, as it has a small therapeutic window (0.6–1.2 mM) and a low toxic dose (~2 mM) (98). Cash et al. (98)

developed a rapid and accurate sensing scheme to monitor therapeutic Li^+ concentrations using PA-based nanosensors that were sensitive to lithium in the dosage range and capable of detecting in vivo lithium changes within 15 s in mouse models (Figure 4a). Lee et al. (22) created PA nanosensors capable of monitoring the concentrations of potassium, which is known to surround tumors at higher concentrations and has been shown to have immune-suppressor qualities (99).

AuNPs are also used for PA-based sensing applications (100). This is because the PA signal can be induced by the LSPR effect of the AuNPs where the optical absorption is orders of magnitude higher than organic fluorophores. Moreover, the resonance wavelength of the NP is tunable by the size and morphology of the AuNPs. This control enables researchers to align NP resonance frequency within the “biological window” (650–1,100 nm), the range in which the least blood and tissue attenuation occurs, thus allowing deeper tissue imaging (100). Applications using this technique include sensing of glutathione (101, 102), epidermal growth factor receptor (103), and miRNA 155 (104). Luke et al. (103) used AuNPs to detect the overexpression of epidermal growth factor receptor, which is typically associated with several types of cancers, for identifying lymph node metastases. With AuNPs, micrometastases as small as 50 μm in size were detectable. Cao et al. (104) developed nanosensors for the accurate PA detection of miRNA-155, which is over-expressed in breast cancer at low concentrations (25 nM). The AuNPs are surface modified with polyethylene glycol (PEG) and two DNA hairpin structures that are partially complementary to each other. In the presence of miRNA-155, the AuNPs formed aggregates due to the hybridization of the opened DNA hairpins by the miRNA and generated a discernable PA signal at the tumor site. Tumor detection in mice was successful two days after sensor inoculation, and the progress of chemotherapy was successfully monitored over the course of 20 days (Figure 4b).

Semiconducting polymer nanoprobes (SPNs), which can generate strong PA signals and are resistant to photodegradation and oxidation (105), are another class of NPs currently used in PA-based sensing. SPNs have already been used to sense oxidative species (105, 106) and pH (107). Lyu et al. (106) fabricated a reaction-based SPN to sense protein sulfenic acids in the tumors of living mice, which are created by the cells in response to oxidative stress. Miao et al. (107) used SPNs as PA reporters for in vivo detection of pH in mice (Figure 4c) to measure aberrant pH levels associated with a multitude of health issues, including tumors, which are surrounded by an acidic environment.

Although AuNPs and SPNs are the most prevalent in PA sensing, other NPs are also being explored. This includes research into human serum albumin- and bovine serum albumin-based NPs for pH sensing (108,109), porphyrin-based NPs for temperature monitoring (110), and NPs from the self-assembly of molecular probes for furin detection (111). Chen et al. (108, 109) used two dyes, benzo[α]phenoxazine (BPOx) and IR-825, that induced the creation of an albumin-based nanoprobe capable of detecting low pH. Dragulescu-Andrasi et al. (111) created an enzymatic-sensitive probe to detect furin and furin-like activity, which is believed to play a major role in tumor progression.

PA sensing is a new field with many applications, but there remain challenges that must be addressed. A major challenge is the trade-off in choosing the optimal size of the AuNP to be used. NPs that are too small (<10 nm) will not accumulate sufficiently for imaging because they will be quickly cleared from the bloodstream by the kidney (97), whereas NPs larger than 10 nm are not easily cleared from the bloodstream, which may lead to long-term toxicity (97,103). Some researchers have used the lymphatic system by injecting the known cancer with the NPs and allowing them to move with the interstitial fluid into the lymphatic system (103) to address clearance issues. The challenge of NP clearance must be addressed before the widespread application of NPs in the clinical setting can be achieved. Even with these challenges, PA sensing offers new and exciting avenues of chemical sensing, including combinations with other imaging techniques such as MRI.

MULTIMODAL NANOSENSORS

Nanosensors, based on each individual signal-transduction mechanism discussed above, have their own sets of advantages and challenges for applications in biological systems. Therefore, it is natural to develop synergistic nanosensors with multiple modalities by combining several signal transduction mechanisms to overcome the individual challenges. Indeed, several nanosensors described in the previous sections are themselves multimodal probes (46, 94, 98, 106). For instance, fluorescence and PA naturally work in parallel in multimodal sensing schemes, as acoustic signals are often evoked by the thermal energy generated during the photon absorptions of the surrounding fluorophores. Lyu et al. (106) have demonstrated that their protein sulfenic acid PA nanoprobes can also provide fluorescence emission with high spatial resolution, therefore complementing the PA sensing schemes (Figure 5). The peptide-based nanosensors developed by Lin et al. (46) for thrombin detection also have dual modalities: fluorescence mode for in vivo monitoring and mass spectroscopy mode through ex vivo urinal analysis of the cleaved peptide segments. Some plasmonic nanoconstructs are also capable of simultaneous SERS and PA sensing, as recently demonstrated by Köker et al. (112). They demonstrated self-assembly of plasmonic NPs by fluorescent protein fragments to create local hotspots for both Raman and PA imaging. MRI-based nanosensors can be further combined with upconverted luminescence (UCL) sensing modality, as Liu et al. (94) have demonstrated in the drug release monitoring platform. MRI and UCL can both track drug release processes and cross-check with each other to minimize potential interferences. Modification of MRI-based nanoprobes to include fluorescence components can be useful for dual-mode detection, as shown by the high-fluorine nanoprobes Zhang et al. (113) fabricated for breast tumor detection through 19F MRI and fluorescence imaging. Finally, all metal NP-based nanosensors used for in vivo applications are potential dual-modal probes, as electron microscopies can be applied in postmortem studies to correlate the location and organization of the sensors with functional dynamics illuminated by the other sensing mode.

CONCLUSIONS AND OUTLOOK

Nanosensors have received much attention in recent years in the biological sciences as part of the tool kit to better understand the dynamics of biological processes of fundamental importance. In this review, we aim to capture some of the significant developments of

imaging-based nanosensors over the past five years, narrated on the basis of different signal transduction mechanisms. There is ample evidence that compared to molecular or bulk counterparts, nanoscale materials provide more degrees of freedom in rational sensor designing by leveraging their advantageous physiochemical properties and unique biological interactions (114). However, the design and functional complexity nanobiosensors offer can be both a blessing and an impediment to general sensor development, due to the myriad interactions at the nano-bio interface (115). Therefore, there is strong impetus in the nanoscience community to formulate an array of standardized characterization protocols, similar to the well-established tests for molecular sensors (116). This effort would enable researchers to establish performance benchmarks and facilitate comparisons of different sensor prototypes, therefore paving the way for nanosensor commercialization with better quality controls (117). We believe that one of the ultimate goals for nanosensor development is to completely illuminate the chemistry of the body, therefore correlating different biological processes on a much larger length scale. Given the extremely rapid advancement of nanosensors, that day may not be far in the future.

ACKNOWLEDGMENTS

This work was supported by grants R01 NS081641, R01 EB024186, UF1 NS107713, and OT2 OD024909 from the US National Institutes of Health (NIH) to H.A.C. The authors thank Dr. Isen Calderon for the vigorous editing and insightful feedback during the writing of the manuscript.

DISCLOSURE STATEMENT

The authors are not aware of any affiliations, memberships, funding, or financial holdings that might be perceived as affecting the objectivity of this review.

LITERATURE CITED

1. Kim SJ, Choi SJ, Jang JS, Cho HJ, Kim ID. 2017 Innovative nanosensor for disease diagnosis. Acc. Chem. Res 50:1587–96 [PubMed: 28481075]
2. Rong G, Corrie SR, Clark HA. 2017 In vivo biosensing: progress and perspectives. ACS Sens. 2:327–38 [PubMed: 28723197]
3. Pantelopoulos A, Bourbakis NG.2010A survey on wearable sensor-based systems for health monitoring and prognosis. IEEE Trans. Syst. Man Cybern. C 40:1–12
4. Borisov SM, Wolfbeis OS. 2008 Optical biosensors. Chem. Rev 108:423–61 [PubMed: 18229952]
5. Song S, Qin Y, He Y, Huang Q, Fan C, Chen HY. 2010 Functional nanoprobes for ultrasensitive detection of biomolecules. Chem. Soc. Rev 39:4234–43 [PubMed: 20871878]
6. Peng HS, Chiu DT. 2015 Soft fluorescent nanomaterials for biological and biomedical imaging. Chem. Soc. Rev 44:4699–722 [PubMed: 25531691]
7. Bandokar AJ, Jeang WJ, Ghaffari R, Rogers JA. 2019 Wearable sensors for biochemical sweat analysis. Annu. Rev. Anal. Chem 12:1–22
8. Ma F, Li Y, Tang B, Zhang CY. 2016 Fluorescent biosensors based on single-molecule counting. Acc. Chem. Res 49:1722–30 [PubMed: 27583695]
9. Kresge N, Simoni RD, Hill RL. 2006 The chemistry of fluorescent indicators: the work of Roger Y. Tsien. J. Biol. Chem 281:29–31
10. Paredes RM, Etzler JC, Watts LT, Zheng W, Lechleiter JD. 2008 Chemical calcium indicators. Methods 46:143–51 [PubMed: 18929663]
11. Santos-Figueroa LE, Moragues ME, Climent E, Agostini A, Martínez-Máñez R, Sancenón F. 2013 Chromogenic and fluorogenic chemosensors and reagents for anions. A comprehensive review of the years 2010–2011. Chem. Soc. Rev 42:3489–613 [PubMed: 23400370]

12. Lin MZ, Schnitzer MJ. 2016 Genetically encoded indicators of neuronal activity. Nat. Neurosci 19:1142–53 [PubMed: 27571193]
13. Lamy CM, Sallin O, Loussert C, Chatton JY. 2012 Sodium sensing in neurons with a dendrimer-based nanoprobe. ACS Nano 6:1176–87 [PubMed: 22288942]
14. Kim EH, Chin G, Rong G, Poskanzer KE, Clark HA. 2018 Optical probes for neurobiological sensing and imaging. Acc. Chem. Res 51:1023–32 [PubMed: 29652127]
15. Meyer D, Hagemann A, Kruss S. 2017 Kinetic requirements for spatiotemporal chemical imaging with fluorescent nanosensors. ACS Nano 11:4017–27 [PubMed: 28379687]
16. Shi JY, Tian F, Lyu J,Yang M. 2015 Nanoparticle based fluorescence resonance energy transfer (FRET) for biosensing applications. J. Mater Chem. B 3:6989–7005
17. Sahari A, Ruckh TT, Hutchings R, Clark HA. 2015 Development of an optical nanosensor incorporating a pH-sensitive quencher dye for potassium imaging. Anal. Chem 87:10684–87 [PubMed: 26444247]
18. Du X, Xie X. 2017 Non-equilibrium diffusion controlled ion-selective optical sensor for blood potassium determination. ACS Sens. 2:1410–14 [PubMed: 28949507]
19. Morales JM, Skipwith CG, Clark HA. 2015 Quadruplex integrated DNA (QuID) nanosensors for monitoring dopamine. Sensors 15:19912–24 [PubMed: 26287196]
20. Walsh R, Morales JM, Skipwith CG, Ruckh TT, Clark HA. 2015 Enzyme-linked DNA dendrimer nanosensors for acetylcholine. Sci. Rep 5:14832 [PubMed: 26442999]
21. Cash KJ, Clark HA. 2012 *In vivo* histamine optical nanosensors. Sensors 12:11922–32 [PubMed: 23112690]
22. Lee CH, Folz J, Zhang W, Jo J, Tan JWY, et al. 2017 Ion-selective nanosensor for photoacoustic and fluorescence imaging of potassium. Anal. Chem 89:7943–49 [PubMed: 28633520]
23. Rong G, Kim EH, Poskanzer KE, Clark HA. 2017 A method for estimating intracellular ion concentration using optical nanosensors and ratiometric imaging. Sci. Rep 7:10819 [PubMed: 28883429]
24. Huang X, Song J, Yung BC, Huang X, Xiong Y, Chen X. 2018 Ratiometric optical nanoprobes enable accurate molecular detection and imaging. Chem. Soc. Rev 47:2873–920 [PubMed: 29568836]
25. Rong GX, Kim EH, Qiang Y, Di WJ, Zhong YD, et al. 2018 Imaging sodium flux during action potentials in neurons with fluorescent nanosensors and transparent microelectrodes. ACS Sens. 3:2499–505 [PubMed: 30358986]
26. Waxman SG, Dib-Hajj S, Cummins TR, Black JA. 1999 Sodium channels and pain. PNAS 96:7635–39 [PubMed: 10393872]
27. Qiang Y, Seo KJ, Zhao XY, Artoni P, Golshan NH, et al. 2017 Bilayer nanomesh structures for transparent recording and stimulating microelectrodes. Adv. Funct. Mater 27:1704117
28. Bachilo SM, Strano MS, Kittrell C, Hauge RH, Smalley RE, Weisman RB. 2002 Structure-assigned optical spectra of single-walled carbon nanotubes. Science 298:2361–66 [PubMed: 12459549]
29. Zhang J, Boghossian AA, Barone PW, Rwei A, Kim JH, et al. 2011 Single molecule detection of nitric oxide enabled by d(AT)15 DNA adsorbed to near infrared fluorescent single-walled carbon nanotubes. J.Am. Chem. Soc 133:567–81 [PubMed: 21142158]
30. Iverson NM, Barone PW, Shandell M, Trudel LJ, Sen S, et al. 2013 *In vivo* biosensing via tissue-localizable near-infrared-fluorescent single-walled carbon nanotubes. Nat. Nanotechnol 8:873–80 [PubMed: 24185942]
31. Kruss S, Salem DP, Vukovic L, Lima B, Vander Ende E, et al. 2017 High-resolution imaging of cellular dopamine efflux using a fluorescent nanosensor array. PNAS 114:1789–94 [PubMed: 28179565]
32. Hu J, Wang ZY, Li CC, Zhang CY. 2017 Advances in single quantum dot-based nanosensors. Chem. Commun 53:13284–95
33. Wegner KD, Hildebrandt N. 2015 Quantum dots: bright and versatile *in vitro* and *in vivo* fluorescence imaging biosensors. Chem. Soc. Rev 44:4792–834 [PubMed: 25777768]

34. van Sark WGJHM Frederix PLTM, Van den Heuvel DJ, Gerritsen HC, Bol AA, et al. 2001Photooxidation and photobleaching of single CdSe/ZnS quantum dots probed by room-temperature time-resolved spectroscopy. J. Phys. Chem. B 105:8281–84
35. Hildebrandt N, Spillmann CM, Algar WR, Pons T, Stewart MH, et al. 2017 Energy transfer with semiconductor quantum dot bioconjugates: a versatile platform for biosensing, energy harvesting, and other developing applications. Chem. Rev 117:536–711 [PubMed: 27359326]
36. Orte A, Alvarez-Pez JM, Ruedas-Rama MJ. 2013 Fluorescence lifetime imaging microscopy for the detection of intracellular pH with quantum dot nanosensors. ACS Nano 7:6387–95 [PubMed: 23808971]
37. Zamaleeva AI, Collot M, Bahembera E, Tisseyre C, Rostaing P, et al. 2014 Cell-penetrating nanobiosensors for pointillistic intracellular Ca^{2+} -transient detection. Nano Lett. 14:2994–3001 [PubMed: 24754795]
38. Ruckh TT, Skipwith CG, Chang W, Senko AW, Bulovic V, et al. 2016 Ion-switchable quantum dot Förster resonance energy transfer rates in ratiometric potassium sensors. ACS Nano 10:4020–30 [PubMed: 27089024]
39. Chakraborty K, Veetil AT, Jaffrey SR, Krishnan Y. 2016 Nucleic acid-based nanodevices in biological imaging. Annu. Rev. Biochem 85:349–73 [PubMed: 27294440]
40. Saha S, Prakash V, Halder S, Chakraborty K, Krishnan Y. 2015A pH-independent DNA nanodevice for quantifying chloride transport in organelles of living cells. Nat. Nanotechnol 10:645–51 [PubMed: 26098226]
41. Tay CY, Yuan L, Leong DT. 2015 Nature-inspired DNA nanosensor for real-time *in situ* detection of mRNA in living cells. ACS Nano 9:5609–17 [PubMed: 25906327]
42. Chen F, Bai M, Cao K, Zhao Y, Cao X, et al. 2017 Programming enzyme-initiated autonomous DNAzyme nanodevices in living cells. ACS Nano 11:11908–14 [PubMed: 29045785]
43. Wei W, He X, Ma N. 2014 DNA-templated assembly of a heterobivalent quantum dot nanoprobe for extra- and intracellular dual-targeting and imaging of live cancer cells. Angew. Chem. Int. Ed 53:5573–77
44. Peng R, Zheng X, Lyu Y, Xu L, Zhang X, et al. 2018 Engineering a 3D DNA-logic gate nanomachine for bispecific recognition and computing on target cell surfaces. J. Am. Chem. Soc 140:9793–96 [PubMed: 30021431]
45. He L, Lu D, Liang H, Xie S, Zhang X, et al. 2018 mRNA-initiated, three-dimensional DNA amplifier able to function inside living cells. J. Am. Chem. Soc 140:258–63 [PubMed: 29211455]
46. Lin KY, Kwong GA, Warren AD, Wood DK, Bhatia SN. 2013 Nanoparticles that sense thrombin activity as synthetic urinary biomarkers of thrombosis. ACS Nano 7:9001–9 [PubMed: 24015809]
47. Dudani JS, Ibrahim M, Kirkpatrick J, Warren AD, Bhatia SN. 2018 Classification of prostate cancer using a protease activity nanosensor library. PNAS 115:8954–59 [PubMed: 30126988]
48. Wang C, Li X, Zhang F.2016 Bioapplications and biotechnologies of upconversion nanoparticle-based nanosensors. Analyst 141:3601–20 [PubMed: 26978012]
49. Liu Y, Chen M, Cao T, Sun Y, Li C, et al. 2013Acyanine-modified nanosystem for *in vivo* upconversion luminescence bioimaging of methylmercury. J.Am. Chem. Soc 135:9869–76 [PubMed: 23763640]
50. Yu Q, Gao P, Zhang KY, Tong X, Yang H, et al. 2017 Luminescent gold nanocluster-based sensing platform for accurate H_2S detection *in vitro* and *in vivo* with improved anti-interference. Light Sci. Appl 6:e17107 [PubMed: 30167221]
51. Sun XC, Lei Y. 2017 Fluorescent carbon dots and their sensing applications. Trends Anal. Chem 89:163–80
52. Galyean AA, Behr MR, Cash KJ. 2018 Ionophore-based optical nanosensors incorporating hydrophobic carbon dots and a pH-sensitive quencher dye for sodium detection. Analyst 143:458–65 [PubMed: 29226289]
53. Mahou P, Vermot J, Beaurepaire E, Supatto W. 2014 Multicolor two-photon light-sheet microscopy. Nat. Methods 11:600–1 [PubMed: 24874570]
54. Xu S, Cui J, Wang L. 2016 Recent developments of low-toxicity NIR II quantum dots for sensing and bioimaging. Trends Anal. Chem 80:149–55

55. Yi M, Yang S, Peng Z, Liu C, Li J, et al. 2014 Two-photon graphene oxide/aptamer nanosensing conjugate for *in vitro* or *in vivo* molecular probing. Anal. Chem 86:3548–54 [PubMed: 24592855]
56. Wan H, Yue J, Zhu S, Uno T, Zhang X, et al. 2018 A bright organic NIR-II nanofluorophore for three-dimensional imaging into biological tissues. Nat. Commun 9:1171 [PubMed: 29563581]
57. Fan Y, Wang P, Lu Y, Wang R, Zhou L, et al. 2018 Lifetime-engineered NIR-II nanoparticles unlock multiplexed in vivo imaging. Nat. Nanotechnol 13:941–46 [PubMed: 30082923]
58. Suhling K, Hirvonen LM, Levitt JA, Chung P-H, Tregidgo C, et al. 2015 Fluorescence lifetime imaging (FLIM): basic concepts and some recent developments. Med. Photonics 27:3–40
59. Niehörster T, Loschberger A, Gregor I, Kramer B, Rahn HJ, et al. 2016Multi-target spectrally resolved fluorescence lifetime imaging microscopy. Nat. Methods 13:257–62 [PubMed: 26808668]
60. Shi J, Zhou M, Gong A, Li Q, Wu Q, et al. 2016 Fluorescence lifetime imaging of nanoflares for mRNA detection in living cells. Anal. Chem 88:1979–83 [PubMed: 26813157]
61. Zhang KY, Zhang J, Liu Y, Liu S, Zhang P, et al. 2015 Core-shell structured phosphorescent nanoparticles for detection of exogenous and endogenous hypochlorite in live cells via ratiometric imaging and photoluminescence lifetime imaging microscopy. Chem. Sci 6:301–7 [PubMed: 28757940]
62. Howes PD, Chandrawati R, Stevens MM. 2014 Colloidal nanoparticles as advanced biological sensors. Science 346:1247390 [PubMed: 25278614]
63. Lee TH, Lapidus LJ, Zhao W, Travers KJ, Herschlag D, Chu S. 2007 Measuring the folding transition time of single RNA molecules. Biophys. J 92:3275–83 [PubMed: 17307831]
64. Zvyagin AV, Sreenivasan VKA, Goldys EM, Panchenko VY, Deyev SM. 2015 Photoluminescent hybrid inorganic-protein nanostructures for imaging and sensing in vivo and in vitro In *Bio-Synthetic Hybrid Materials and Bionanoparticles: A Biological Chemical Approach Towards Material Science*, ed. Boker A, van Rijn P, pp. 245–84. RSC: Cambridge, UK
65. Guo LH, Jackman JA, Yang HH, Chen P, Cho NJ, Kim DH. 2015 Strategies for enhancing the sensitivity of plasmonic nanosensors. Nano Today 10:213–39
66. Taylor AB, Zijlstra P. 2017 Single-molecule plasmon sensing: current status and future prospects. ACS Sens. 2:1103–22 [PubMed: 28762723]
67. Storhoff JJ, Lazarides AA, Mucic RC, Mirkin CA, Letsinger RL, Schatz GC. 2000 What controls the optical properties of DNA-linked gold nanoparticle assemblies? J. Am. Chem. Soc 122:4640–50
68. Jain PK, Huang WY, El-Sayed MA. 2007 On the universal scaling behavior of the distance decay of plasmon coupling in metal nanoparticle pairs: a plasmon ruler equation. Nano Lett. 7:2080–88
69. Rong G, Wang H, Reinhard BM. 2010 Insights from a nanoparticle minuet: two-dimensional membrane profiling through silver plasmon ruler tracking. Nano Lett. 10:230–38 [PubMed: 20017502]
70. Rong GX, Reinhard BM. 2012 Monitoring the size and lateral dynamics of ErbB1 enriched membrane domains through live cell plasmon coupling microscopy. PLOS ONE 7:e34175 [PubMed: 22470534]
71. Feizpour A, Stelter D, Wong C, Akiyama H, Gummuluru S, et al. 2017 Membrane fluidity sensing on the single virus particle level with plasmonic nanoparticle transducers. ACS Sens. 2:1415–23 [PubMed: 28933537]
72. Chen T, Hong Y, Reinhard BM. 2015 Probing DNA stiffness through optical fluctuation analysis of plasmon rulers. Nano Lett. 15:5349–57 [PubMed: 26121062]
73. Sun M, Xu L, Fu P, Wu X, Kuang H, et al. 2016 Scissor-like chiral metamolecules for probing intracellular telomerase activity. Adv. Funct. Mater 26:7352–58
74. Li M, Cushing SK, Wu N.2015 Plasmon-enhanced optical sensors: a review. Analyst 140:386–406 [PubMed: 25365823]
75. Xu J, Yu H, Hu Y, Chen M, Shao S. 2016 A gold nanoparticle-based fluorescence sensor for high sensitive and selective detection of thiols in living cells. Biosens. Bioelectron 75:1–7 [PubMed: 26278044]

76. Lio DCS, Liu C, Wiraja C, Qiu B, Fhu CW, et al. 2018Molecular beacon gold nanosensors for leucinerich alpha-2-glycoprotein-1 detection in pathological angiogenesis. ACS Sens. 3:1647–55 [PubMed: 30095245]
77. Wu P, Hwang K, Lan T, Lu Y. 2013 A DNAzyme-gold nanoparticle probe for uranyl ion in living cells. J. Am. Chem. Soc 135:5254–57 [PubMed: 23531046]
78. Zhu D, Zhao DX, Huang JX, Li J, Zuo XL, et al. 2018 Protein-mimicking nanoparticle (Protmin)-based nanosensor for intracellular analysis of metal ions. Nucl. Sci. Tech 29:5
79. Gu X, Trujillo MJ, Olson JE, Camden JP. 2018 SERS sensors: recent developments and a generalized classification scheme based on the signal origin. *Annu.* Rev. Anal. Chem 11:147–69
80. Harmsen S, Bedics MA, Wall MA, Huang R, Detty MR, Kircher MF. 2015 Rational design of a chalcogenopyrylium-based surface-enhanced resonance Raman scattering nanoprobe with attomolar sensitivity. Nat. Commun 6:6570 [PubMed: 25800697]
81. Haun JB, Yoon TJ, Lee H, Weissleder R. 2010 Magnetic nanoparticle biosensors. Wiley Interdiscip. Rev. Nanomed. Nanobiotechnol 2:291–304 [PubMed: 20336708]
82. Blümich B 2016 Introduction to compact NMR: a review of methods. Trends Anal. Chem 83:2–11
83. Zabow G, Dodd SJ, Koretsky AP. 2015 Shape-changing magnetic assemblies as high-sensitivity NMR-readable nanoprobes. Nature 520:73–77 [PubMed: 25778701]
84. Liu G, Gao J, Ai H, Chen X. 2013 Applications and potential toxicity of magnetic iron oxide nanoparticles. Small 9:1533–45 [PubMed: 23019129]
85. Nakamura Y, Mochida A, Choyke PL, Kobayashi H. 2016 Nanodrug delivery: Is the enhanced permeability and retention effect sufficient for curing cancer? Bioconjug. Chem 27:2225–38 [PubMed: 27547843]
86. Lee N, Yoo D, Ling D, Cho MH, Hyeon T, Cheon J. 2015 Iron oxide based nanoparticles for multi-modal imaging and magnetoresponsive therapy. Chem. Rev 115:10637–89 [PubMed: 26250431]
87. Luo Y, Kim EH, Flask CA, Clark HA. 2018 Nanosensors for the chemical imaging of acetylcholine using magnetic resonance imaging. ACS Nano 12:5761–73 [PubMed: 29851460]
88. Okada S, Bartelle BB, Li N, Breton-Provencher V, Lee JJ, et al. 2018 Calcium-dependent molecular fMRI using a magnetic nanosensor. Nat. Nanotechnol 13:473–77 [PubMed: 29713073]
89. Angelovski G 2017 Heading toward macromolecular and nanosized bioresponsive MRI probes for successful functional imaging. Acc. Chem. Res 50:2215–24 [PubMed: 28841293]
90. Berridge MJ. 2014 Calcium regulation of neural rhythms, memory and Alzheimer's disease. J. Physiol 592:281–93 [PubMed: 23753528]
91. Yuan Y, Ge S, Sun H, Dong X, Zhao H, et al. 2015 Intracellular self-assembly and disassembly of 19F nanoparticles confer respective "off" and "on" 19F NMR/MRI signals for legumain activity detection in zebrafish. ACS Nano 9:5117–24 [PubMed: 25868488]
92. Gallo J, Kamaly N, Lavdas I, Stevens E, Nguyen QD, et al. 2014 CXCR4-targeted and MMP-responsive iron oxide nanoparticles for enhanced magnetic resonance imaging. Angew. Chem. Int. Ed 53:9550–54
93. Liow SS, Dou Q, Kai D, Li Z, Sugiarto S, et al. 2017 Long-term real-time in vivo drug release monitoring with AIE thermogelling polymer. Small 13:1603404
94. Liu J, Bu J, Bu W, Zhang S, Pan L, et al. 2014 Real-time in vivo quantitative monitoring of drug release by dual-mode magnetic resonance and upconverted luminescence imaging. Angew. Chem. Int. Ed 53:4551–55
95. Schellenberger E 2010 Bioresponsive nanosensors in medical imaging. J. R. Soc. Interface 7(Suppl. 1):S83–91 [PubMed: 19846442]
96. Reinhardt CJ, Chan J. 2018 Development of photoacoustic probes for *in vivo* molecular imaging. Biochemistry 57:194–99 [PubMed: 29022344]
97. Lemaster JE, Jokerst JV. 2017 What is new in nanoparticle-based photoacoustic imaging? Wiley Interdiscip. Rev. Nanomed. Nanobiotechnol 9:1404
98. Cash KJ, Li C, Xia J, Wang LV, Clark HA. 2015 Optical drug monitoring: photoacoustic imaging of nanosensors to monitor therapeutic lithium *in vivo*. ACS Nano 9:1692–98 [PubMed: 25588028]

99. Eil R, Vodnala SK, Clever D, Klebanoff CA, Sukumar M, et al. 2016 Ionic immune suppression within the tumour microenvironment limits T cell effector function. Nature 537:539–43 [PubMed: 27626381]
100. Li W, Chen X. 2015 Gold nanoparticles for photoacoustic imaging. Nanomedicine 10:299–320 [PubMed: 25600972]
101. Yasmin Z, Khachatryan E, Lee YH, Maswadi S, Glickman R, Nash KL. 2015 *In vitro* monitoring of oxidative processes with self-aggregating gold nanoparticles using all-optical photoacoustic spectroscopy. Biosens. Bioelectron 64:676–82 [PubMed: 25441418]
102. Liu Y, Yang Z, Huang X, Yu G, Wang S, et al. 2018 Glutathione-responsive self-assembled magnetic gold nanowreath for enhanced tumor imaging and imaging-guided photothermal therapy. ACS Nano 12:8129–37 [PubMed: 30001110]
103. Luke GP, Myers JN, Emelianov SY, Sokolov KV. 2014 Sentinel lymph node biopsy revisited: ultrasound-guided photoacoustic detection of micrometastases using molecularly targeted plasmonic nanosensors. Cancer Res. 74:5397–408 [PubMed: 25106426]
104. Cao W, Gao W, Liu Z, Hao W, Li X, et al. 2018 Visualizing miR-155 to monitor breast tumorigenesis and response to chemotherapeutic drugs by a self-assembled photoacoustic nanoprobe. Anal. Chem 90:9125–31 [PubMed: 29961324]
105. Pu K, Shuhendler AJ, Jokerst JV, Mei J, Gambhir SS, et al. 2014 Semiconducting polymer nanoparticles as photoacoustic molecular imaging probes in living mice. Nat. Nanotechnol 9:233–39 [PubMed: 24463363]
106. Lyu Y, Zhen X, Miao Y, Pu K. 2017 Reaction-based semiconducting polymer nanoprobes for photoacoustic imaging of protein sulfenic acids. ACS Nano 11:358–67 [PubMed: 27997794]
107. Miao Q, Lyu Y, Ding D, Pu K. 2016 Semiconducting oligomer nanoparticles as an activatable photoacoustic probe with amplified brightness for in vivo imaging of pH. Adv. Mater 28:3662–68 [PubMed: 27000431]
108. Chen Q, Liu X, Chen J, Zeng J, Cheng Z, Liu Z. 2015 A self-assembled albumin-based nanoprobe for in vivo ratiometric photoacoustic pH imaging. Adv. Mater 27:6820–27 [PubMed: 26418312]
109. Chen Q, Liu X, Zeng J, Cheng Z, Liu Z. 2016 Albumin-NIR dye self-assembled nanoparticles for photoacoustic pH imaging and pH-responsive photothermal therapy effective for large tumors. Biomaterials 98:23–30 [PubMed: 27177219]
110. Ng KK, Shakiba M, Huynh E, Weersink RA, Roxin A, et al. 2014 Stimuli-responsive photoacoustic nanoswitch for *in vivo* sensing applications. ACS Nano 8:8363–73 [PubMed: 25046406]
111. Dragulescu-Andrasi A, Kothapalli SR, Tikhomirov GA, Rao J, Gambhir SS. 2013Activatable oligomerizable imaging agents for photoacoustic imaging of furin-like activity in living subjects. J. Am. Chem. Soc 135:11015–22 [PubMed: 23859847]
112. Köker T, Tang N, Tian C, Zhang W, Wang X, et al. 2018 Cellular imaging by targeted assembly of hot-spot SERS and photoacoustic nanoprobes using split-fluorescent protein scaffolds. Nat. Commun 9:607 [PubMed: 29426856]
113. Zhang C, Moonshi SS, Wang W, Ta HT, Han Y, et al. 2018 High F-content perfluoropolyether-based nanoparticles for targeted detection of breast cancer by 19F magnetic resonance and optical imaging. ACS Nano 12:9162–76 [PubMed: 30118590]
114. Nel AE, Madler L, Velegol D, Xia T, Hoek EM, et al. 2009 Understanding biophysicochemical interactions at the nano-bio interface. Nat. Mater 8:543–57 [PubMed: 19525947]
115. Björnmalm M, Faria M, Caruso F. 2016 Increasing the impact of materials in and beyond bio-nano science. J. Am. Chem. Soc 138:13449–56 [PubMed: 27672703]
116. Gooding JJ, Bakker E, Kelley S, Long Y, Merkx M, et al. 2017 Should there be minimum information reporting standards for sensors? *ACS* Sens. 2:1377–79 [PubMed: 29073765]
117. Faria M, Björnmalm M, Thurecht KJ, Kent SJ, Parton RG, et al. 2018 Minimum information reporting in bio-nano experimental literature. Nat. Nanotechnol 13:777–85 [PubMed: 30190620]

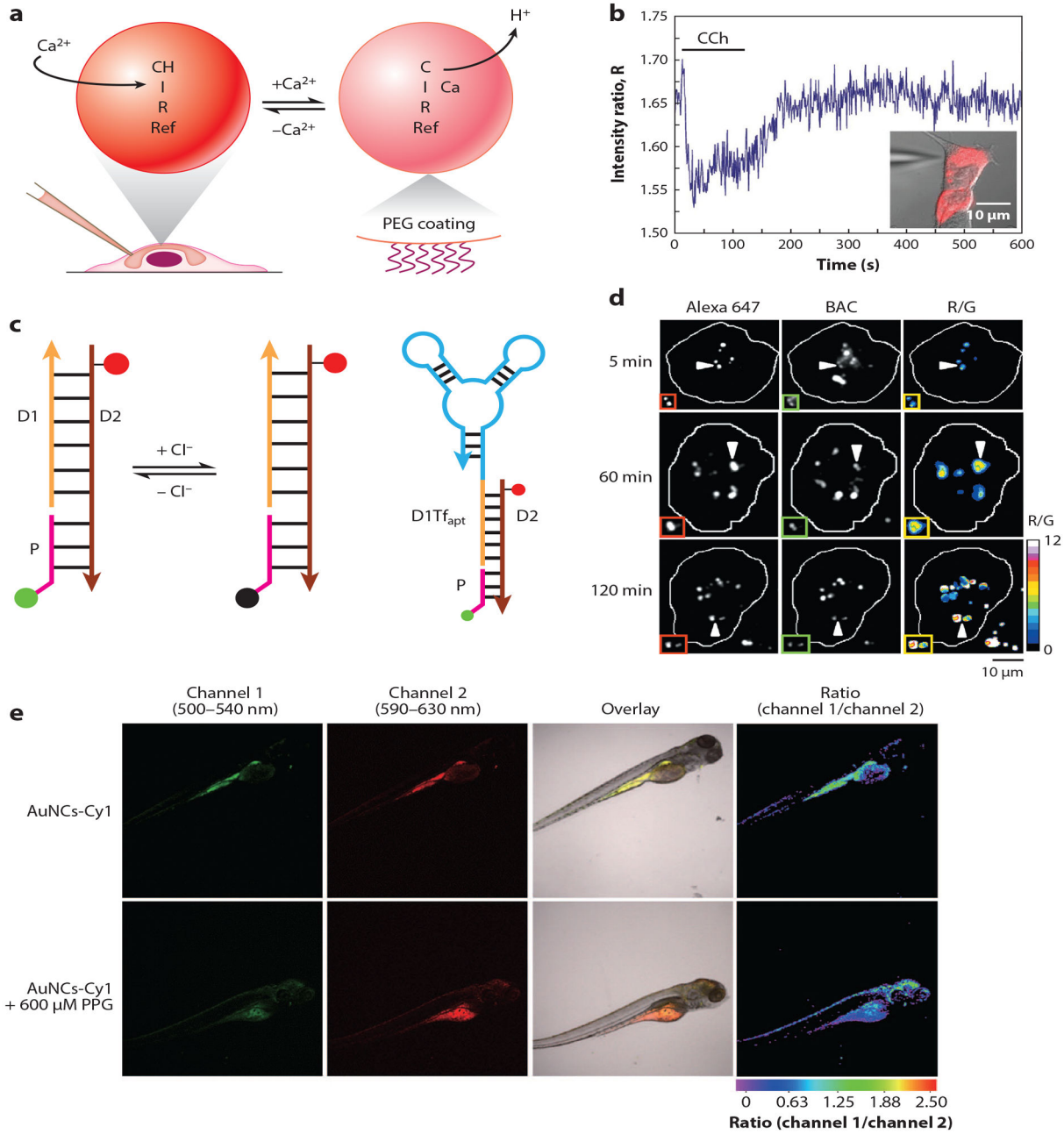

Figure 1.

Fluorescence-based nanosensors. (*a*) Optode-based sensing scheme. The selective extraction of Ca^{2+} by the ionophore (I) induces deprotonations of two pH-sensitive fluorophores, chromoionophore (CH) and rhodamine (Ref), to maintain charge neutrality within the sensor matrix. Polyethylene glycol (PEG)-coated nanosensors were introduced to the intracellular space through microinjection.(*b*) Ratiometric sensor response to calcium flux in the HeLa cell stimulated by carbachol (CCh). Adapted from Reference 23.(c) Structure and working mechanism of Clensor. Cl^- sensitive fluorophore (*green*) on the sensing module (*pink*) undergoes collisional quenching in the presence of Cl^-, while Alexa 647 (*red*) fluorescence on the normalizing module (*brown*) is independent from Cl^-. The targeting module (*orange*)

links to an RNA aptamer (*cyan*) targeting transferrin receptor in the cellular recycling pathway.(*d*) Pseudocolor R/G maps of Clensor-labeled haemocytes from *Drosophila* at different time points along the endolysosomal pathway. Adapted with permission from Reference 40. Copyright 2015, Springer Nature. (*e*) Dual-color and ratiometric confocal images of zebrafish after injection of gold nanoclusters (AuNCs) functionalized with merocyanine derivative (Cy1) for endogenous H_2S sensing. (*e, top)* Control group. (*e, bottom)* Sensor ratiometric response to the zebrafish treated by propargylglycine (PPG) for endogenous H_2S inhibition. Adapted with permission from Reference 50. Copyright 2017, Springer Nature.

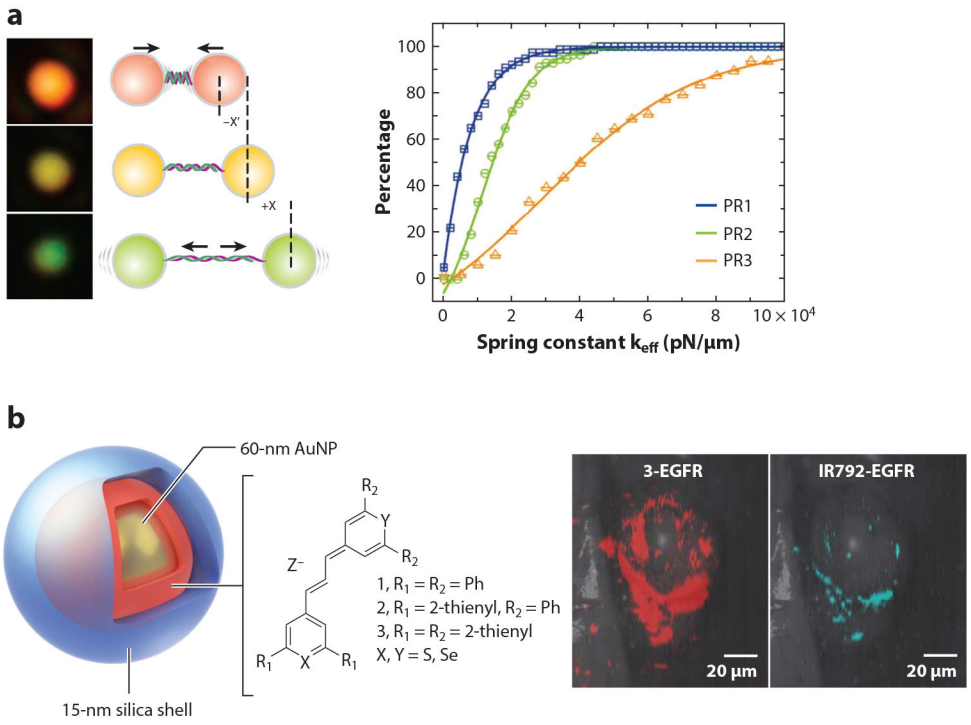

Figure 2.

Plasmonics-based nanosensors. (*a, left*) DNA stiffness can be quantified by the spectral shift of DNA-tethered gold nanoparticles (plasmon rulers). (*a, right)* Cumulative distribution plot of calculated DNA spring constants of three different plasmon rulers (PR1–3). Adapted with permission from Reference 72. Copyright 2015, American Chemical Society. (*b, left*) Schematic drawing of the SERS Au nanoprobe. A 60-nm AuNP is coated by a 15-nm silica shell containing chalcogenopyrylium dye. (*b, right)* Raman images of tumor-targeted SERS nanoprobes in mice. The chalcogenopyrylium dye 3 (*red*) and the IR792-based SERS nanoprobes were conjugated with anti-EGFR and then injected to the mice with xenograft tumors via tail vein. The chalcogenopyrylium-based probe offered three-times-higher signal. Adapted with permission from Reference 80. Copyright 2015, Springer Nature.

Abbreviations: AuNP, gold nanoparticle; EGFR, epidermal growth factor receptor; SERS, surface-enhanced Raman scattering.

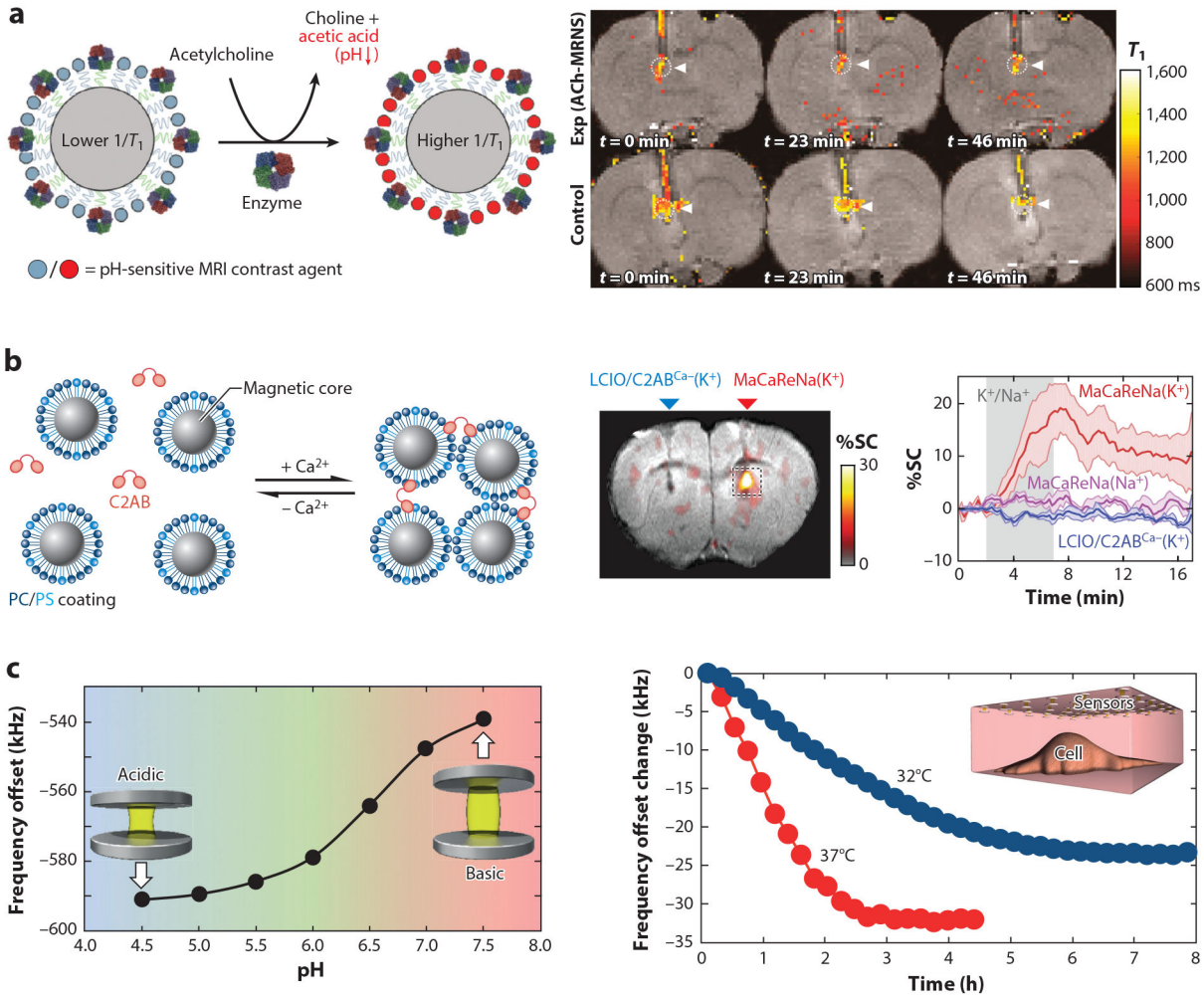

Figure 3.

MRI-based nanosensors. (*a, left*) ACh nanosensor scheme. The enzymatic hydrolysis of the ACh generates a local pH change that leads to the increased T_1 relaxation rate of the pH-sensitive contrast agent on the sensor. (*a, right)* MRI images showing ACh detections by the nanosensors at different time points. Nanosensors were delivered through cannula with (*top row*) and without (*bottom row*) clozapine administration. Adapted with permission from Reference 87. Copyright 2018, American Chemical Society. (*b, left)* Design of magnetic calcium-responsive NPs based on iron oxide lipid-coated NP and fused C2AB. (*b, right)* MRI image and SC time course show MRI sensor responses during 100-mM K^+ infusion compared with control groups. Adapted with permission from Reference 88. Copyright 2018, Springer Nature. (*c, left)* Nickel-based sensor has the pH-dependent NMR shifts due to the expansion (shrinkage) of the pH-sensitive hydrogel spacer at high (low) pH within physiological range. (*c, right*) NMR frequency of the sensor array shifts due to the acidification of MDCK cell surroundings (*inset*) via cell CO_2 production and necrosis under two temperatures. Different response profiles are indicative different cell metabolic rates. Adapted with permission from Reference 83. Copyright 2015, Springer Nature.

Abbreviations: ACh, acetylcholine; C2AB, C2 calcium-binding domains of synaptotagmin 1; MDCK, Madin-Darby canine kidney; MRI, magnetic resonance imaging; NMR, nuclear

magnetic resonance; NP, nanoparticle; PC/PS, phosphatidylcholine/phosphatidylserine; SC, signal change.

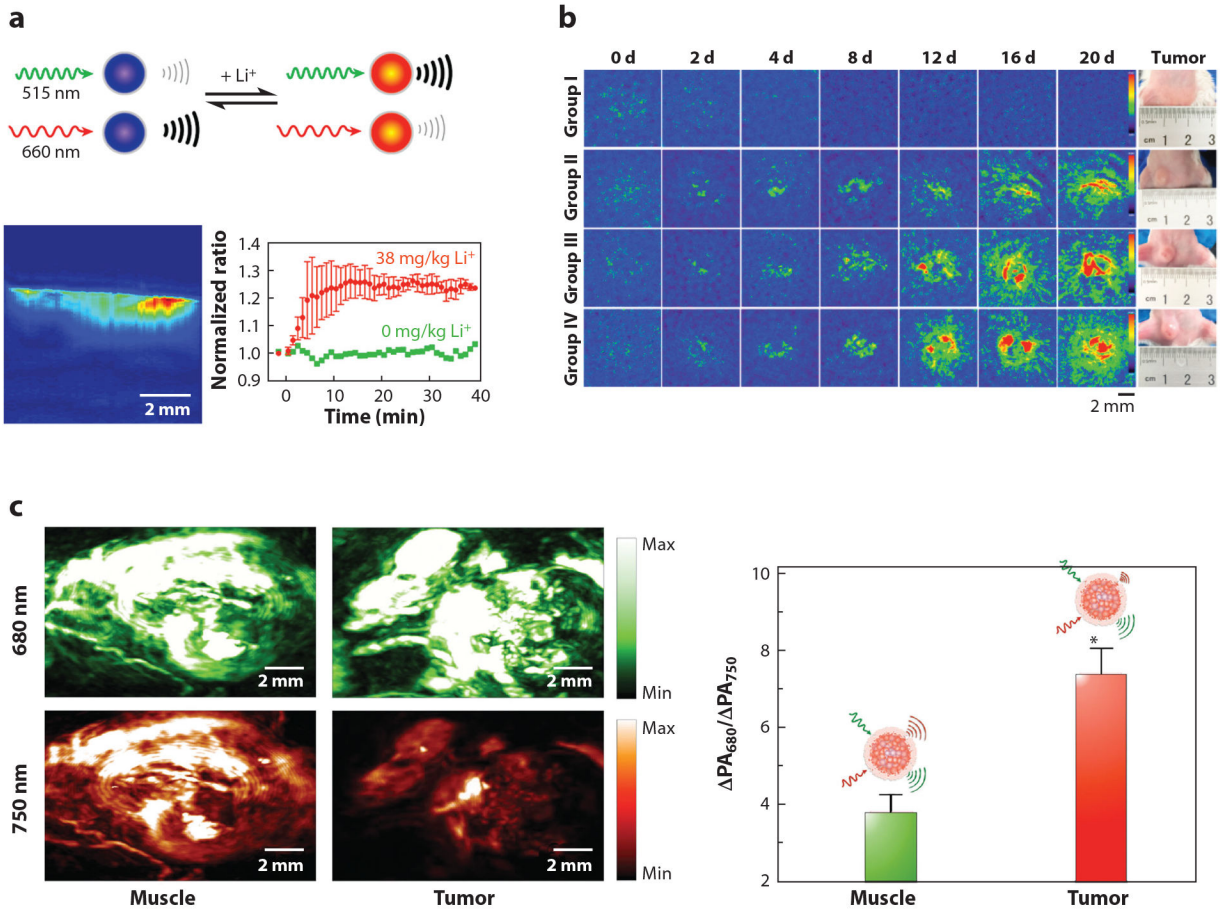

Figure 4.

Photoacoustics-based nanosensors. (*a, top*) Mechanism of dual-wavelength photoacoustic (PA) imaging for lithium detection. PA signals from each wavelength change as a function of lithium concentration. (*a, bottom)* Depth profile and dynamic changes of PA signals of lithium sensors at the injection site of the mouse. Sensor response to lithium administration with a peak time of 14 min. Adapted with permission from Reference 98. Copyright 2015, American Chemical Society. (*b*) Self-assembled PA nanoprobes for miRNA-155 expression level monitoring for drug efficacy evaluation. Mice in groups I, II, and III were treated with anticancer drug starting at day (d) 0, 4, or 12 after tumor inoculation. Untreated group IV served as a control. Adapted with permission from Reference 104. Copyright 2018, American Chemical Society. (*c*) Dual channel PA images of locally administrated semiconducting oligomer nanoprobes at the muscle and tumor (*left*) and their ratiometric readout (*right*) of the PA intensity increments at respective wavelengths ($\Delta PA_{680}/\Delta PA_{750}$). Adapted with permission from Reference 107. Copyright 2016, John Wiley and Sons.

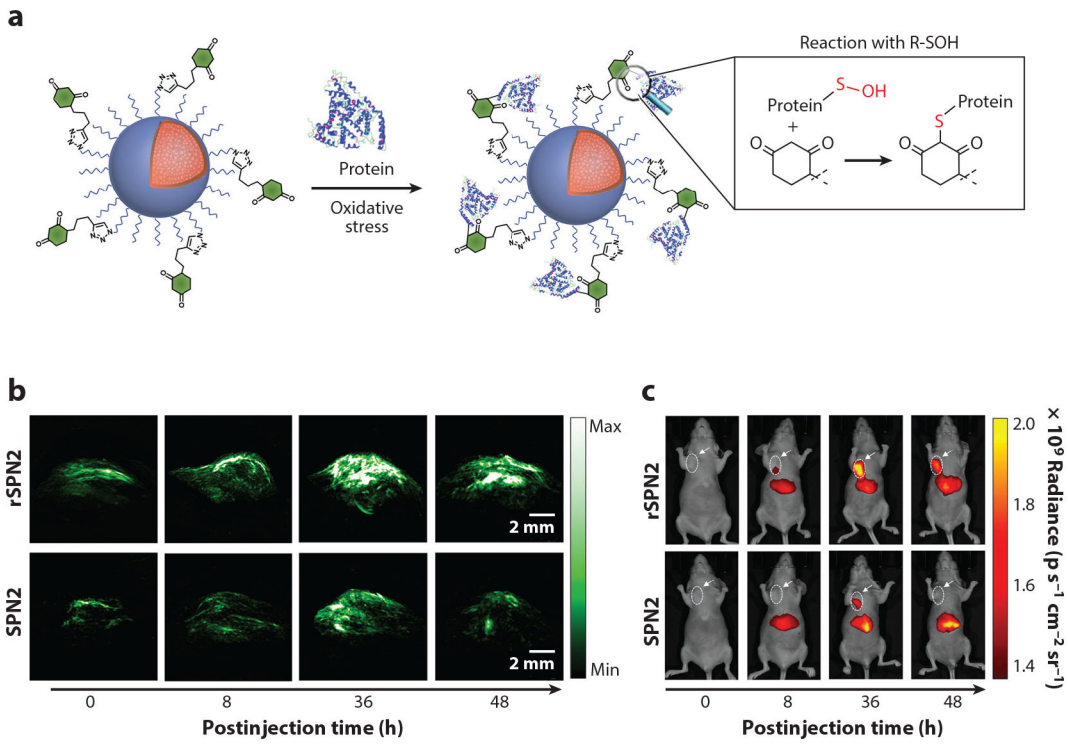

Figure 5.

Multimodal nanosensors. (*a*) Mechanism of the recognition reaction between semiconducting polymer nanoprobes (SPNs) and protein-bound sulfenic acids. Images from fluorescence (*b*) and photoacoustic (*c*) mode of reaction-based semiconductor polymer nanoprobes (rSPN2) and SPN2 (control group) for sulfenic acid detection at different time points at the tumor sites of the living mice. Nanoprobes were administrated through tail vein injection. Adapted with permission from Reference 106. Copyright 2017, American Chemical Society.